Short circuit current distribution analysis using a network model based on a 5x5 primitive matrix

Paulo M. De Oliveira-De Jesus[b,*], Andrés A. Rojas Quintana[1]

[a]Electrical and Electronic Engineering Department, School of Engineering, Los Andes University, Bogotá, Colombia
[b]Transener, Buenos Aires, Argentina

Summary

This paper analyzes the well known short-circuit current distribution problem in electric distribution facilities from a new perspective. Fault current distribution, temporary overvoltages and ground potential rise are determined according to a detailed network model based on 5x5 primitive matrices. The methodology is suitable to be applied either by using any closed-form expression for the self and mutual impedance of the ground loop -such as the Carson's modified formula- or by incorporating network parameters adjusted by dynamic state estimation tools and synchronized measurements. The proposed method was illustrated in a simple radial two-bus and also applied on a large-scale 115/12kV system with 360 nodes. Results were compared and validated against the exact nodal admittance approach provided by the OpenDSS platform under the same modeling conditions (modified Carson approach). Since traditional 4x4 primitive matrix models lack of a explicit ground loop impedance representation, it is encouraged the use and further development of the proposed methodology in systems with widespread deployment of phasor measurement units.

Keywords: Short-circuit analysis, current distribution, ground potential rise, neutral to earth voltages

1. Introduction

Advanced short-circuit analysis is required not only to determine the fault current magnitude to be handled by the equipment in substations but also to assess how that current is distributed through the returning paths. Fault currents flowing through earth in substations and towers will provoke a ground potential rises (GPR) and temporary overvoltages (TOV) that could endanger the personal safety and security of the system. Temporary potentials arise until the fault is duly cleared by the protection system. The assessment of magnitudes and duration of perturbations should be depicted by advanced short-circuit analyses.

This kind of studies can be performed resorting to approximated network models based upon symmetrical components [1, 2] or exact calculations over a phase-domain framework [2]. Table 1 lists a number of advanced power flow and short circuit with different network models.

Most of advanced power system analyses -power flow, short-circuit and state estimation- are founded on a 4x4 primitive matrix network model [3]. In this representation, hereinafter denoted "4x4" models, impedance equations for multiphase and neutrals/ground are usually corrected using a ground return impedance model and later reduced to an equivalent 4x4 matrix using the Kron's formula.

In this instance, self and mutual impedances are finally described as a three phase (*abc*) and neutral (*n*) representation. Several short-circuit solution approaches for fault current distribution have been introduced under the "4x4" paradigm, i.e. double-sided elimination method [5], driving-point impedance technique [6], ladder circuit solution [7–9], single division factor [10], two-port theory [11] and nodal admittance methods [12–15]. Special purpose application software such as OpenDSS [15], WinIGS [16] and CDEGS [17] include specific modules to determine current fault distribution in substations and lines. Other general purpose application tools such as EMTP [18–21] and PSPICE: [22] have been also used to tackle the problem.

*Corresponding Author at: Electrical and Electronic Engineering Department, School of Engineering, Los Andes University, Bogotá, Colombia, Tel.:+57 3182566629.

Email addresses: `pm.deoliveiradejes@uniandes.edu.co` (Paulo M. De Oliveira-De Jesus), `andres.rojas@transener.com.ar` (Andrés A. Rojas Quintana)

URL: `https://power.uniandes.edu.co/pdeoliveira` (Paulo M. De Oliveira-De Jesus)

Table 1: Summary of network models suitable to be used in advanced short-circuit analysis

Reference	Network Model		
	Seq: 0+-	4x4	5x5
IEEE80 [1]	◦		
Meliopoulos [2]	◦	◦	
Dawalibi [5]		◦	
Gooi [6]		◦	
Popovic [7]		◦	
Levey [8, 9]		◦	
Kiessling [10]		◦	
Buccheri [11]		◦	
Zou [12]		◦	
Penido [13, 14]		◦	
OpenDSS [15]		◦	
WinIGS [16]		◦	
CDEGS [17]		◦	
Klucznik [18]		◦	
Acharya [19, 21]		◦	
Oka [20]		◦	
Chen [22]		◦	
Kersting [3]		◦	◦
Anderson [23]		◦	◦
Ciric [24, 25, 27]			◦

Another possible mathematical description of the network is the complete primitive model [23], hereafter referred as ”5x5”. In this model three-phase and neutral impedances are calculated without any correction due to earth effect and the fifth wire (the resistance and reactance of the ground loop) is intended to represent a fictitious ground conductor. As a result, the ”5x5” model comprises an equivalent of three phases (*abc*), neutral (*n*) and grounding (*g*) impedance representation. This model has been recently applied by [24–26] to perform system studies such as such as power flow, optimal power flow and state estimation. In [27], the model developed in [24] is used to calculate short-circuit current distribution. However, in this valuable contribution results about the fault current division, produced GPR and TOV were not compared and validated with any existing procedure.

The impedance of the ground return path exhibits a non-linear frequency dependence. The problem of how current carrying wires are affected by the ground effect was solved in 1926 by Carson [4]. The exact calculation of ground path impedances generally requires the evaluation of an infinite complex integral. Today, the integral evaluation using numerical integration could require considerable computational times [28]. Several approximate closed-form expressions for the integral have been proposed such as the standard Carson’s series formula (generally taken as reference) [4], Deri formula [29], Gary-Dubanton formulas [30], Alvarado-Betancourt formulas [31], Noda’s double symmetry-plane formulas [32] and the widespread used Carson’s modified series formula [2]. Some recent research has shown that the standard Carson-series method can produce large errors as high as 7.7% with respect to the evaluation of a infinite complex integral [28]. Other methods could produce errors between 8-15%.

It is worth to recall that Carson considered the return current through the earth with uniform resistivity and to be of infinite extent. This assumption leads to a fixed resistance of 0.0953 ohm/mile at 60 Hz [33]. Even though closed-form equations have been sufficiently precise to design and operate existing power systems [34], those assumptions should be reappraised in the context of next generation distribution systems with higher short circuit levels due to increased penetration of distributed generators. These systems are characterized by having short and untransposed line sections, and high resistivity variability [26].

Nowadays, the deployment of phasor measurement units (PMU) in power grids are enabling synchronized voltages and branch currents measurements [35]. PMU can also provide synchronized measurements of currents in neutral and shield wires [36, 37]. The increased observability gave by the PMU infrastructure could improve the estimation line impedance parameters, including self and mutual impedances of the ground loop [26]. This means that traditional earth approximations can be adjusted to real-wold conditions considering a full observable distribution system. Under this perspective, the use of 5x5 primitive matrices with PMU estimated parameters in advanced short-circuit studies is worth.

In this paper a detailed network model is applied to determine the ground potential rise, temporary overvoltages and fault current distribution through all returning paths. The proposal was illustrated in a radial two-bus and tested on a large-scale system. Results obtained were compared and validated against the approximate sequence domain analysis and the exact model based upon ”4x4” nodal admittance approach provided by the OpenDSS platform [15].

The paper is organized in the following manner. Section 2 presents the methodology. Results obtained from two case studies are discussed and compared with standard sequence network analysis in Section 3. Conclusions are drawn in Section 4.

2. Methodology

2.1. The 5x5 primitive matrix network model

The detailed network model developed in [26] is structured according to a three-phase line segment with equivalent neutral wire grounded at both sending i and receiving nodes k is shown in Fig. 1. The 5x5 primitive impedance matrix $\mathbf{z_{ik}}$ of length 1 unit between nodes 0 and 1 is given by:

$$\mathbf{z_{ik}} = \begin{bmatrix} z_{ik}^{aa} & z_{ik}^{ab} & z_{ik}^{ac} & z_{ik}^{an} & z_{ik}^{ag} \\ z_{ik}^{ba} & z_{ik}^{bb} & z_{ik}^{bc} & z_{ik}^{bn} & z_{ik}^{bg} \\ z_{ik}^{ca} & z_{ik}^{cb} & z_{ik}^{cc} & z_{ik}^{cn} & z_{ik}^{cg} \\ z_{ik}^{na} & z_{ik}^{nb} & z_{ik}^{nc} & z_{ik}^{nn} & z_{ik}^{ng} \\ z_{ik}^{ga} & z_{ik}^{gb} & z_{ik}^{gc} & z_{ik}^{gn} & z_{ik}^{gg} \end{bmatrix} \quad (1)$$

The model depicted in Fig. 1 has explicit representation for the ground loop, then self and mutual phase and neutral parameters of $\mathbf{z_{ik}}$ are determined without ground effect. According to [3] self and mutual impedances of phases in Ω/mile without Carson's corrections are:

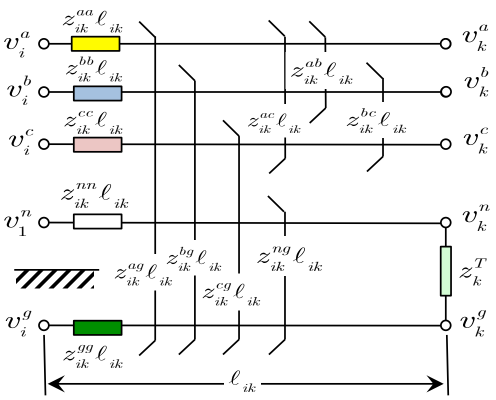

Figure 1: Two-terminal distribution line segment line

$$z_{ik}^{qq} = r_{ik}^{qq} + k\log_e\left(\frac{1}{D_{ik}^{qq}}\right)i \quad (2)$$

$$z_{ik}^{pq} = k\log_e\left(\frac{1}{D_{ik}^{pq}}\right)i \quad (3)$$

$$\forall q, p = a, b, c, n \quad (4)$$

where $i=\sqrt{-1}$ and,

r_{ik}^{qq} is the resistance of phase or neutral conductor in Ω/mile,

D_{ik}^{qq} is the geometric mean radius of phase or neutral conductors in feet.

D_{ik}^{pq} is the distance between two different conductors in feet.

Factor k is equal to $4\pi f\xi\times10^{-4} = f\mu_0$ in Ω/miles where μ_0 is the permeability in free space in H/mile, with ξ=1.609. Frequency f is given in Hz.

Network parameters of Eq. 1 can be adjusted to real world conditions by means of a dynamic system state estimator based upon synchronized phasor measurements [26, 36].

The estimation process can include in the measurement vector and the state of the system vector all tower or pole footing resistances z_k^T. The impedance of the ground path z_{ik}^{gg} should be estimated using the Carson integral [28]. However, this procedure is expensive in computer times. Instead, several approximate closed-form expressions such as the Deri formula [29], Gary-Dubanton formulas [30], Alvarado-Betancourt formulas [31], Noda's double symmetry-plane formulas [32] can be used.

In this paper, self and mutual impedances of the ground path in Ω/mile are defined according to traditional modified Carson's representation (equivalent depth of return method) [2]:

$$z_{ik}^{gg} = \frac{1}{4}\pi k + k\log_e\left(\frac{D_e}{h^{qg}}\right)i \quad \forall q = a, b, c, n \quad (5)$$

where the parameter D_e=$2160\sqrt{\frac{\rho}{f}}$ is the equivalent distance in feet and the h^{qg} is the height between phase/neutral conductors and the equivalent ground conductor in feet. This basic representation allow us to validate the proposal with standard sequence-based methods [2] and nodal admittance methods [15].

The coupling between phase/neutral wires and the ground path is given by the following equation:

$$z_{ik}^{qg} = \frac{1}{2}\left(z_{ik}^{gg} + z_{ik}^{qq} - \bar{z}_{ik}^{qq}\right) \quad \forall q = a, b, c, n \quad (6)$$

where the parameter $\bar{z}_{ik}^{qq}$ is the phase self-impedance corrected by Carson equations [3]:

$$\bar{z}_{ik}^{qq} = r_{ik}^{qq} + \frac{1}{2}\pi k + k\left(\log_e \frac{D_e}{D_{ik}^{qq}}\right)i \quad (7)$$
$$\forall q = a, b, c, n$$

Consider a general system with m nodes as shown in Fig. 2. The voltage source is reserved for the line segment 0-1. It comprises an ideal voltage source $\mathbf{V_0}$ and its equivalent Thévenin impedance matrix $\mathbf{z_{S01}}$. Nodes from 2 to m are regarded as load or generation nodes. So, the smallest number of nodes is m=2 with a voltage source at sending node 1 and a load/generation unit at the receiving node 2.

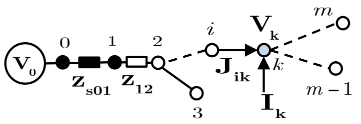

Figure 2: m segment network topology

The relationship between nodal voltages and branch currents can be established according to Kirchhoff laws by equation 10:

$$\mathbf{V} = \mathbf{V_0} - \mathbf{T}^T \cdot \text{blkdiag}(\mathbf{z}) \cdot \mathbf{J} \tag{8}$$

where $\mathbf{V}=[\mathbf{v_1}, \ldots, \mathbf{v_k}, \ldots \mathbf{v_m}]^T$ is the $(5m-5) \times 1$ state of the system vector on which each element of $\mathbf{V}$ is denoted a $\mathbf{v_k} = [v_k^a, v_k^b, v_k^c, v_k^n, v_k^g]^T$. The source voltage is defined as a $(5m-5)\times 1$ vector: $\mathbf{V_0}=[\mathbf{v_0}, \ldots, \mathbf{v_0}]^T$ where $\mathbf{v_0}=[v_0^a, v_0^b, v_0^c, v_0^n, v_0^g]^T$. The set of all primitive matrices are $\mathbf{z}=[\mathbf{z_{01}}, \mathbf{z_{12}} \ldots, \mathbf{z_{ik}} \ldots, \mathbf{z_{m-1,m}}]^T$. The operator `blkdiag` returns a block diagonal matrix based on specified square blocks.

The branch current vector is defined as follows:

$$\mathbf{J} = -\mathbf{T} \cdot \mathbf{M} \cdot \mathbf{I} \tag{9}$$

where is defined as $\mathbf{J}=[\mathbf{j_{01}}, \ldots, \mathbf{j_{ik}}, \ldots, \mathbf{j_{m-1,m}}]^T$. $\mathbf{I}=[\mathbf{i_1}, \ldots, \mathbf{i_k}, \ldots \mathbf{i_m}]^T$ is the $(5m-5) \times 1$ injected current vector, where $\mathbf{i_k} = [i_k^a, i_k^b, i_k^c, i_k^u, i_k^u]^T$. Injected currents i_k^a, i_k^b, i_k^c will depend on fault current component i_{sck}^a, the line capacitance charging i_{ck}^a and the loading/distributed generation model adopted at each phase i_{lk}^a. For instance, at phase a, the injected current is $i_k^a = i_{sck}^a + i_{ck}^a + i_{lk}^a$. Entry i_k^u of $\mathbf{i_k}$is the unbalanced or fault current that is flowing through neutrals and earth paths ($-i_k^a$-i_k^b-i_k^c). Matrix $\mathbf{M}$ groups the neutral to earth current divisors and $\mathbf{T}$ is the topology matrix built according the numbering scheme shown in Fig. 2. Both matrices $\mathbf{M}$ and $\mathbf{T}$ have the same dimension $(5m-5) \times (5m-5)$ and should be structured according to the procedure established in [26]. When substituting Eq. 9 in 10, we can observe that $\mathbf{T}^T \cdot \texttt{blkdiag}(\mathbf{z}) \cdot \mathbf{T} \cdot \mathbf{M}$ is a constant $(5m-5) \times (5m-5)$ impedance matrix, unique for each circuit:

$$\mathbf{Z} = \mathbf{T}^T \cdot \text{blkdiag}(\mathbf{z}) \cdot \mathbf{T} \cdot \mathbf{M} \tag{10}$$

All vectors and matrices defined above have complex entries. Matrix $\mathbf{Z}$ can account the effect of neighboring circuits or parallel lines using appropriate Kron's reductions. Thus, the complete 5x5 primitive matrix model relating voltages and currents yields to the general Kirchhoff expression:

$$\mathbf{V} = \mathbf{V_0} + \mathbf{Z} \cdot \mathbf{I} \tag{11}$$

2.2. *Short-circuit analysis - m nodes*

Under steady-state conditions, given the load/generation profile at each bus k=1,...,m, the solution of the set of $5m-5$ equations with $5m-5$ unknowns provide us the so-called power flow solution at unbalanced operation. If a fault occurs at given node k and phase p, the system can be easily solvable by introducing additional equations and state variables. For instance, a single phase to neutral fault at given phase p and node k through a resistance R_f must satisfy an additional equation $v_k^p - v_k^n = R_f \cdot i_{sck}^p$ where the short-circuit current i_{sck}^p should be regarded as an additional unknown variable.

The system posed in Eq. 11 is non-linear if injected currents (i_k^a, i_k^b, i_k^c) are represented as voltage dependent loads such as constant power, ZIP or exponential. In this case, power flow solution under steady state or fault conditions is straightforward by using any solver such as Newton. Otherwise, if injected load currents are linear the set equations given in Eq. 11 has direct solution and no iterative-based method is necessary.

Once the Eq. 11 is solved, the short-circuit current distribution is given by Eq. 9. The grid to earth current at each node k is given by:

$$i_k^{ng} = \frac{v_k^n - v_k^g}{z_k^T} \quad \forall k = 2, \ldots, m \tag{12}$$

The ground potential rise (GPR) is a temporary overvoltage that appears between local neutrals and remote earth until the fault is effectively cleared. It can be defined as the maximum electrical potential that a ground grid may attain relative to a distant grounding point assumed to be at the potential of remote earth. This voltage, GPR is equal to the maximum grid current multiplied by the grid resistance [1].

$$GPR_k = i_k^{ng} z_k^T \quad \forall k = 2, \ldots, m \tag{13}$$

The coefficient of grounding (COG) [38] indicates the ratio (expressed as a percentage), of the highest root-mean square (rms) line-to-ground power-frequency temporary overvoltage on a sound phase with respect to the power frequency nominal line-to-line voltage in all nodes, during a fault to ground affecting one or more phases of the system. The limit established in [38] for a system be considered effectively grounded is 80%.

$$COG_k = \frac{v_k^a}{v_0} = \frac{v_k^b}{v_0} = \frac{v_k^c}{v_0} \quad \forall k = 2, \ldots, m \tag{14}$$

where v_0 is the nominal voltage of the system.

To illustrate the proposal, in the following detailed formulation and solution approaches for short-circuit distribution and ground potential rise calculations are provided for two test systems. Due to space limitations only single-phase to neutral faults are considered.

2.3. *Short-circuit analysis - Two nodes system*

In this case, the number of nodes is m=2. Fig. illustrates two line sections. The first segment 0-1 is reserved for the equivalent power source associated with the upstream substation. The second segment 1-2 corresponds to a three-phase line of length ℓ_{12}.

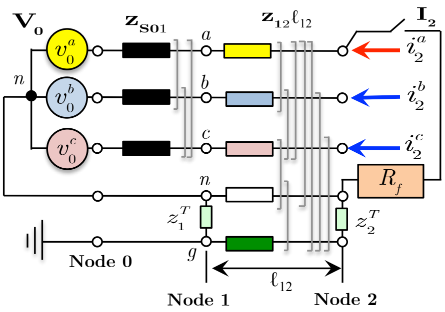

Figure 3: Two-node system with a single phase to neutral fault

2.3.1. *Two node model description*

According to the general model specified in Eq. 10, the detailed matrix formulation for short-circuit current calculation is given by Eq. 16:

$$\mathbf{v_2} = \mathbf{v_0} + \mathbf{Z} \cdot \mathbf{i_2} \tag{15}$$

in matrix notation,

$$\begin{bmatrix} v_2^a \\ v_2^b \\ v_2^c \\ v_2^n \\ v_2^g \end{bmatrix} = \begin{bmatrix} v_0^a \\ v_0^b \\ v_0^c \\ v_0^n \\ v_0^g \end{bmatrix} + \mathbf{Z} \begin{bmatrix} i_2^a \\ i_2^b \\ i_2^c \\ i_2^u \\ i_2^u \end{bmatrix} \tag{16}$$

where the system matrix $\mathbf{Z}$ has a dimension of 5×5. The main source is represented by the segment 0-1 through a Thévenin equivalent impedance matrix $\mathbf{z_{S01}}$ and an ideal three-phase voltage source $\mathbf{V_0}$=$[v_0^a, v_0^b, v_0^c, v_0^n, v_0^g]^T$=$[v_0 e^{0i} + v_0^n,\ v_0 e^{\frac{-2\pi}{3}i} + v_0^n,\ v_0 e^{\frac{2\pi}{3}i} + v_0^n,\ v_0^n,\ 0]^T$. Entry v_0 is the line-to-neutral nominal voltage. Entry v_0^n is the neutral voltage at origin with respect to local reference v_0^g which is set equal to 0. Voltage neutral at sending bus v_1^n should be determined from the local ground impedance z_1^T and the sum of all returning ground currents as follows:

$$v_1^n = v_0^n = z_1^T J_{12}^{gg} = z_1^T \frac{v_2^g - v_2^n}{z_2^T} \tag{17}$$

Note that neutral at node 1 depends on grounding resistance value at node 2. This model does not support null grounding impedances.

The Thévenin equivalent impedance $\mathbf{z_{S01}}$ is

$$\mathbf{z_{S01}} = \begin{bmatrix} z_{S01}^{aa} & z_{S01}^{ab} & z_{S01}^{ac} \\ z_{S01}^{ba} & z_{S01}^{bb} & z_{S01}^{bc} \\ z_{S01}^{ca} & z_{S01}^{cb} & z_{S01}^{cc} \end{bmatrix} \tag{18}$$

Parameters of $\mathbf{z_{S01}}$ can be determined from single and three phase short-circuit level as well as by the relations R_1/X_1 and R_0/X_0 at node 1.

The system impedance matrix is given by

$$\mathbf{Z} = (\mathbf{z_{S01}} + \mathbf{z_{12}}) \cdot \mathbf{M} = \mathbf{z_{02}} \cdot \mathbf{M} \tag{19}$$

where the matrix of reduction factors at the line segment 1-2 is:

$$\mathbf{M} = \mathtt{diag}(\begin{bmatrix} 1, & 1, & 1, & 1-\zeta_2, & \zeta_2 \end{bmatrix}) \tag{20}$$

and the reduction factor at node 2 (ζ_2) is

$$\zeta_2 = \frac{i_2^{ng}}{i_2^u} = \frac{z_{12}^{nn}\ell_{12} + z_{12}^{ag}\ell_{12} - z_{12}^{an}\ell_{12} - z_{12}^{ng}\ell_{12}}{z_1^T + z_2^T + z_{12}^{gg}\ell_{12} + z_{12}^{nn}\ell_{12} - 2z_{12}^{ng}\ell_{12}} \tag{21}$$

The injected currents at node 2 ($\mathbf{I_2}$) comprise three components: the load/generation injected current at each phase of node 1, the line charging due to shunt capacitances in the segment 1-2 and the short-circuit currents when the phase $a$is unintentionally connected to a grounded neutral as seen in Fig. 3.

$$\begin{aligned} i_2^a &= i_{l2}^a + i_{c2}^a + i_{sc2}^a \\ i_2^b &= i_{l2}^b + i_{c2}^b \\ i_2^c &= i_{l2}^c + i_{c2}^c \end{aligned}$$

The unbalanced load is written as i_2^u=$-i_2^a - i_2^b - i_2^c$. As the fault is at phase a, only injected current at this phase includes the short-circuit component i_{sc2}^a.

The injected currents at loads are for instance at phase b: $i_{l2}^b = (S_{G2}^b - S_{D2}^b)^* / (v_2^b - v_2^n)^*$, apparent demanded power is given by S_{D2}^b=P_{D2}^b+jQ_{D2}^b and apparent generated power is given by S_{G2}^b=P_{G2}^b+jQ_{G2}^b. For the sake of simplicity, single-phase loads are connected between phase and neutral which general representation is given by the following expression:

$$P_{D2}^b = P_0^b (v_2^b - v_2^n)^\alpha \tag{22}$$

Note that, if α = 0, the model reflects a PQ load; if α = 1, the model reflects a constant current load; and, if α

= 2, the model reflects a constant impedance load. The line capacitance charging model $\mathbf{i_{c2}}$ is obtained from the primitive admittance matrix of section 1-2 $\mathbf{y}_{12}$. Due to lack of space details of how calculate the entries of $\mathbf{y}_{12}$ are omitted. However, a general procedure can be found in [3].

Due space restrictions, only single-phase to neutral fault analysis is considered in this paper.

2.3.2. Single phase to neutral fault

When a single-phase a is unintentionally connected to a grounded neutral through a fault impedance R_f at the faulted node 2, the following conditions should be also added to Eq. 16 to find out the short-circuit currents:

$$v_2^a = R_f i_2^u + v_2^n \tag{23}$$

If the fault impedance R_f=0, then neutral and phase a voltages at node 2 are the same (v_2^a=v_2^n) and the resultant system (Eq. 16 and Eq. 23) has 5 complex equations with 5 complex state variables: the single-phase short circuit current i_{sc2}^a and the voltages v_2^a=v_2^n, v_2^b, v_2^c and v_2^g. Conversely, if the fault impedance R_f ≠0, the resultant system has 6 complex equations with 6 complex state variables: the single-phase short circuit current i_{sc2}^a and the voltages v_2^a, v_2^b, v_2^c, v_2^n and v_2^g.

2.3.3. Solution approach

The system of equations stated in Eq. 16 is non-linear. If system loads are regarded as constant power, then the solution can be assessed through an iterative method. As a special case, if loads are disconnected, the system of equations becomes linear and the solution is direct and no iterative procedure is required. Considering that Z_{ik} is the i,k element of the system impedance $\mathbf{Z}$, the fault impedance R_f=0 and $m_2 = z_1^T/z_2^T$, the direct solution of Eq. 16 is given by Eq. 24.

$$\begin{bmatrix} v_2^a = v_2^n \\ v_2^g \\ v_2^b \\ v_2^c \\ i_{sc2}^a \end{bmatrix} = \begin{bmatrix} m_2+1 & -m_2 & 0 & 0 & Z_{14}+Z_{15}-Z_{11} \\ m_2 & -m_2 & 1 & 0 & Z_{24}+Z_{25}-Z_{21} \\ m_2 & -m_2 & 0 & 1 & Z_{34}+Z_{35}-Z_{31} \\ m_2+1 & -m_2 & 0 & 0 & Z_{44}+Z_{45}-Z_{41} \\ 0 & 1 & 0 & 0 & Z_{54}+Z_{55}-Z_{51} \end{bmatrix}^{-1} \cdot \begin{bmatrix} 1 \\ e^{\frac{-2\pi}{3}i} \\ e^{\frac{2\pi}{3}i} \\ 0 \\ 0 \end{bmatrix} \tag{24}$$

3. Illustrative examples

The proposed short circuit analysis approach was applied to two well-known examples. The first one is the Neutral-to-Earth test system [39]. The second one is the 115/12kV large-scale system included in [2], Chapter 7. Both methods were also solved using the approximate sequence analysis [2] and by the OpenDSS [15] program based upon a detailed 4x4 primitive matrix model.

3.1. NEV system

The NEV test system [39] comprises three-phase with neutral main feeder connected to an ideal 12.47 kV (line-to-line) source. Root and ending nodes have the neutral solidly grounded through a 100 ohms resistance. The test feeder has 6000 ft length with 21 poles. For illustration purposes only one section with two nodes (the source node 1 and the ending node 2) are considered. Single phase to neutral fault is applied at node 2 phase a.

3.1.1. Data setup

System basic characteristics: the phase conductors used are 336,400 26/7 ACSR, GMR = 0.0244 ft., resistance = 0.306 ohm/mile, diameter = 0.721 inches. Neutral Conductor: 4/0 6/1 ACSR: GMR = 0.00814 ft., resistance = 0.592 ohms/mile, diameter = 0.563 inches. The feeder length ℓ_{12} is 1.13 mi long. Impedance at root and remote node are fixed as z_1^T=z_2^T=100 ohms. The test case has an ideal voltage source with $\mathbf{z_{s01}}$=$\mathbf{0}$ (infinite bus). Short circuit analysis at ending node 1 is performed assuming no loads and no shunt admittances $\mathbf{y_{01}}$. Constant power load load at phases b and c are 3500 kVA at 0.95 lagging power factor and 2500 kVA at 0.85 lagging power factor. Line capacitances were neglected. Programs used in the illustrative NEV example were coded in Octave/Matlab. The interested reader can get access to the programs in the following website: https://github.com/pmdeoliveiradejesus/55short-dist.git.

The elements of the primitive matrix $\mathbf{z_{12}}$ in ohm/mile are determined according Eqs 2 - 7 as follows:

$z_{12}^{aa} = z_{12}^{bb} = z_{12}^{cc} = 0.3060 + 0.4506i$,

$z_{12}^{ag} = z_{12}^{bg} = z_{12}^{cg} = z_{12}^{ng}$ = - 0.2043i,
z_{12}^{ab} = - 0.1112i,z_{12}^{ac} = - 0.2361i, z_{12}^{bc} = - 0.1825i,
z_{12}^{an} = - 0.2103i, z_{12}^{bn} = - 0.1762i, z_{12}^{cn} = - 0.1953i,
z_{12}^{nn} = 0.5920 + 0.5838i, z_{12}^{gg} = 0.0953 + 0.5540i.

3.9118 0.3644 0.2520 3.5683 0.0201 The system matrix **Z** is calculated according to Eq. 19 assuming an ideal source at node 1. According to Eq. 21 calculated reduction factor at node 2 (ζ_2) is 0.0034 + 0.0045i.

3.1.2. Case A: single phase a to neutral fault - no loads

In this case, load effect is disregarded. According to Eq. 23, it must be accomplished that: v_2^a=v_2^n with R_f=0. Therefore, equations stated in Eq. 16 are only expressed as a function of system voltages at node 2 and the short-circuit current at phase a through the following system of linear equations:

$$\begin{bmatrix} v_2^a = v_2^n \\ v_2^b \\ v_2^c \\ v_2^n = v_2^a \\ v_2^g \end{bmatrix} = \begin{bmatrix} 1 + v_0^n \\ e^{\frac{-2\pi}{3}i} + v_0^n \\ e^{\frac{2\pi}{3}i} + v_0^n \\ v_0^n \\ v_0^g = 0 \end{bmatrix} + \mathbf{Z} \cdot \begin{bmatrix} i_{sc2}^a \\ 0 \\ 0 \\ -i_{sc2}^a \\ -i_{sc2}^a \end{bmatrix} \tag{25}$$

As the system is linear the solution of Eq. 25 is straightforward. By applying Eq. 24, all voltages at node 2 and the single phase phase current is given by:

$$\begin{bmatrix} v_2^a = v_2^n \\ v_2^g \\ v_2^b \\ v_2^c \\ i_{sc2}^a \end{bmatrix} = \begin{bmatrix} 2084.0\angle -4.86^o \text{ V} \\ 184.0\angle 68.69^o \text{ V} \\ 8551.9\angle -133.68^o \text{ V} \\ 8547.6\angle 130.28^o \text{ V} \\ 3713.7\angle 121.78^o \text{ A} \end{bmatrix} \tag{26}$$

Voltage at neutral's source is determined according to Eq. 27

$$v_1^n = v_2^g - v_2^n = 2081.7\angle 174.61^o \text{ V} \tag{27}$$

The short-circuit current has only one contribution, the power source. Thus, j_{12}^a=- i_{sc2}^a=3713.7 A∠ -58.22^o. Current division at node 2 is shown in the second column of Table 2 and the Fig. 4-a. Note that due to the high local grounding resistance almost 100 % of the fault current is returning through the neutral path. Despite the grid to ground current is quite small (20.8 A), the ground potential rise reaches 2081.7 V at both source and load nodes. As the NEV test system includes high resistances at origin and terminal small currents are able to produce high potential rises. The rise of potential affects non-faulted phases such as v_2^b=8551.9V and v_2^c=8547.6V. In both cases, this result implies a deviation of 68.5% with respect to the nominal line-to neutral voltage. So, the system is effectively grounded since the coefficient of grounding (COG) is below 80 %. If the NEV system is provided with footing resistances lower than 10 ohms, que can observe higher reduction factors and fault currents returning through natural earth.

Solutions obtained using the proposed method are compared with the sequence impedance model provided in Meliopoulos book [2] and validated using the OpenDSS program [15]. Solutions are listed in the third and fourth column of Table 2. The OpenDSS solution is also depicted in Fig. 4-b. The interested reader can verify the solution using the source script included in Appendix A.

We must highlight that both approaches (4x4 and 5x5 models) yield the same solution. Consequently, both approaches are equivalent. The added value of the proposed method stems from the possible inclusion of estimated parameters into the 5x5 primitive matrix.

Table 2 also shows how the sequence model yield inaccurate results with respect to the exact solutions provided by the 5x5 and the OpenDSS model. Thus, from Fig. 5 the connections of sequence networks for a single fault phase to neutral in node 2 is illustrated. The zero-sequence current is 1258.9A∠-57.20^o and the fault current is 3776.7A∠-57.20^o. This latter result is close to the correct one (3713.7∠ -58.22^o). However, the calculated split factor fails. The sequence model dictates that a current of 36.17A is flowing through a 100 ohms resistance at the origin and at the ending node. As a result, the expected GPR (3617 V) is much higher than the correct one (2081.7 V). This result imply an overestimation of the COG of the system.

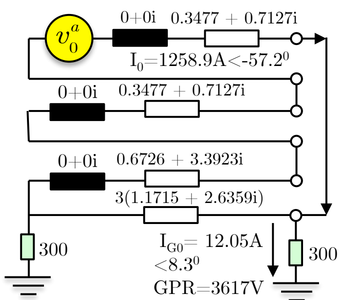

Figure 5: NEV Test System - Sequence networks circuit

3.1.3. Case B: single phase a to neutral fault with PQ loads

This second example assumes the NEV system with two PQ loads at node 2, phase b and c. As the faulted phase a has the same voltage than neutral, it is further

Table 2: Summary of results -NEV system

	Case A: No Loads			Case B: Loads	
	5x5	4x4 [15]	Seq. [2]	5x5	4x4 [15]
j_{12}^a (A)	3713.7	3713.7	3776.8	3911.8	3911.6
j_{12}^b (A)	0	0	-	364.4	364.4
j_{12}^c (A)	0	0	-	252.0	252.0
j_{12}^n (A)	3701.2	3701.1	3741.1	3568.3	3568.3
j_{12}^g (A)	20.817	20.816	36.17	20.061	20.061
COG_2^b	68.5%	68.5%	78.5%	66.0%	66.0 %
COG_2^c	68.5%	68.5%	82.2 %	66.0%	66.0 %
GPR_2 (V)	2081.7	2081.7	3617	2006	2006

assumed that load at node a is not capable absorbe/inject current during the fault. In this case, the system posed in Eq. 28 is non-linear since i_2^b and i_2^c depend on voltages v_2^b and v_2^c, respectively.

$$\begin{bmatrix} v_2^a = v_2^n \\ v_2^b \\ v_2^c \\ v_2^n = v_2^a \\ v_2^g \end{bmatrix} = \begin{bmatrix} 1 + v_0^n \\ e^{\frac{-2\pi}{3}i} + v_0^n \\ e^{\frac{2\pi}{3}i} + v_0^n \\ v_0^n \\ v_0^g = 0 \end{bmatrix} + \mathbf{Z} \cdot \begin{bmatrix} i_{sc2}^a \\ i_2^b \\ i_2^c \\ -i_{sc2}^a - i_2^b - i_2^c \\ -i_{sc2}^a - i_2^b - i_2^c \end{bmatrix} \tag{28}$$

So, there is no direct formula to get the state of the system and the solution is obtained using the the general purpose Matlab's *fmincon* tool.

$$\begin{bmatrix} v_2^a = v_2^n \\ v_2^g \\ v_2^b \\ v_2^c \\ i_{sc2}^a \end{bmatrix} = \begin{bmatrix} 2008.3\angle -6.67^o \text{ V} \\ 174\angle 75.44^o \text{ V} \\ 8238.9\angle -134.64^o \text{ V} \\ 8392.3\angle 128.63^o \text{ V} \\ 3911.7\angle 124.11^o \text{ A} \end{bmatrix} \tag{29}$$

As previously done in the first case A, fifth and sixth column of Table 2 show solutions obtained using the proposed method and the OpenDSS program [15], respectively. If the interested reader want to reproduce the results, loads in the OpenDSS script included in Appendix A can be enabled in order to get the solution of Case B. For the sake of simplicity sequence analysis was omitted. Graphical solution is also presented in Fig. 4-c and Fig. 4-d, for the proposed method and the OpenDSS solution.

In this example both approaches (4x4 and 5x5 models) also yield the same solution. We can observe that the short-circuit level is quite high with respect the one obtained in case A. The reason lies on the contribution of the unbalanced current at load-side. This contribution also produces a lower GPR and COG values.

3.2. Large-scale test case

The proposed method was applied in the 115/12 kV power system used by [2] to compute fault current distribution and ground potential using the sequence model. The system encompass two lines and a substation. The substation is fed by a 25.5 mi long single circuit 115kV sub-transmission line. Loads are fed by a 10 mi long distribution 12 kV circuit. As shown in Fig. 6, the substation has a 115/12 kV 20MVA transformer with delta-wye connection. The subtransmission line comprises 235 towers whose shield wire is solidly grounded through a 30 Ω resistance electrode. The distribution line has 120 poles with neutral wire grounded through a 50 Ω resistance at each pole. In this case, the number of nodes is m=359. The equivalent impedances of the interconnected system are Z_{S01}^+=Z_{S01}^-= 9.8 Ω and Z_{S01}^0= 6.6 Ω. The source station grounding resistance is 2 Ω. At 115/12kV substation, power transformer low voltage neutral as well as incoming shield wires and outgoing neutrals are grounded to a 2 Ω substation ground mat. Soil resistivity is equal to 265 Ωm along the both lines and the substation under study.

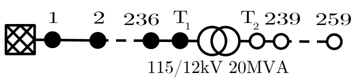

Figure 6: 115/12kV Test system

The GPR and the fault current distribution along the entire system is determined considering a single phase to neutral fault at high-voltage side of the substation (node 238, phase a). Table 3 present the results at node 238.

The solution provided by the 5x5 primitive matrix model matches with the solution provided by the OpenDSS platform. The division factor a=$J_{237-238}^a/i_{237}^{ng}$ is around 57 %. Meliopoulos reported a division fac-

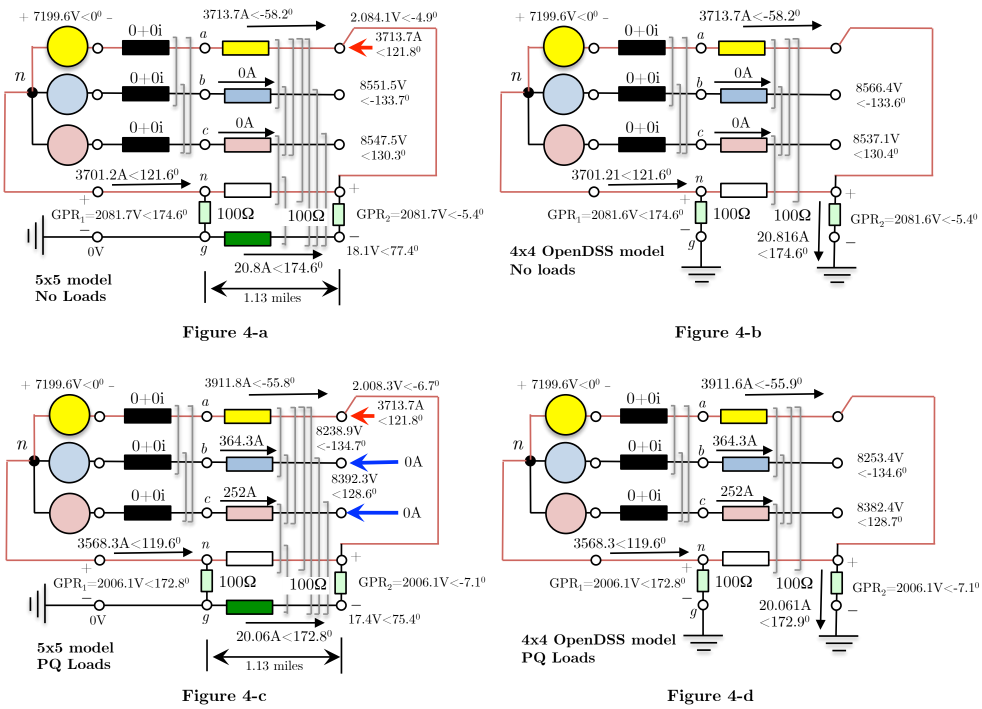

Figure 4: NEV Test System - General solution sketch

Table 3: Summary of results - 115/12kV Test system

Parameters	5x5	4x4 [15]	Seq. [2]
$J^{a}_{237-238}$ (A)	1493.1	1494.2	1470
$J^{n}_{237-238}$ (A)	370.9	371.5	544
$J^{n}_{238-239}$ (A)	279.9	278.2	544
i^{ng}_{237} (A)	852.3	854.4	926
$\|a\|$	57.0 %	57.2 %	63.2 %
GPR_{237} (V)	1704.6	1708.9	1858

tor of 63 % using the approximate sequence model approach [2]. Likewise, we can observe slight differences in the fault current and GPR magnitudes with the approximated sequence model. The fault current distribution patterns for the 5x5 model and the OpenDSS engine are also shown in Figures 7 and 7, respectively.

The GPR magnitude profile for the entire system is shown in Fig. 8. Again, we can observe small differences between both solutions.

The examples discussed in this section aim to validate system solutions with two different network models but with the same earth model assumptions, i.e. modified Carson's equations. The use of detailed 5x5 network models allows to introduce modifications in the primitive matrix by including parameters estimated via enhanced dynamic system state estimation. Further developments of the proposed methodology should be focused on distribution systems with widespread deployment of phasor measurement units.

4. Conclusions

In this paper fault current distribution, temporary overvoltages and ground potential rise are determined according to a detailed network model based on 5x5 primitive matrices. The methodology is suitable to be applied either by using any closed-form expression for the self and mutual impedance of the ground loop -such as the Carson's modified formula- or by incorporating network parameters adjusted by dynamic state estimation tools and synchronized measurements. The proposed method was illustrated in two test systems. The proposed model was validated against the exact nodal admittance approach provided by the OpenDSS platform under the earth modeling conditions.

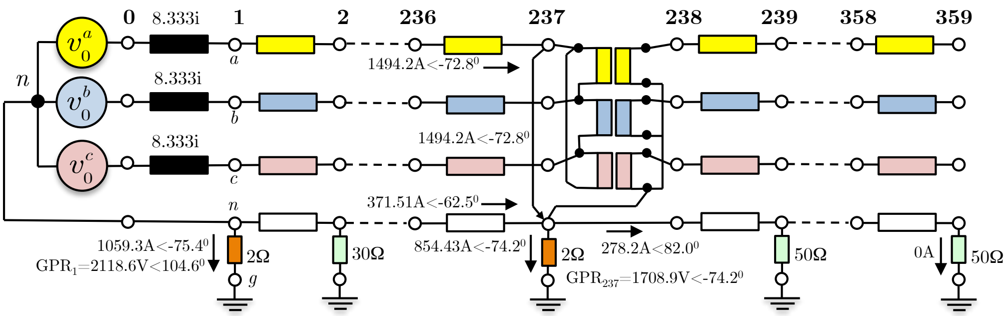

Figure 7: 115/12kV Test system - Fault current distribution (OpenDSS)

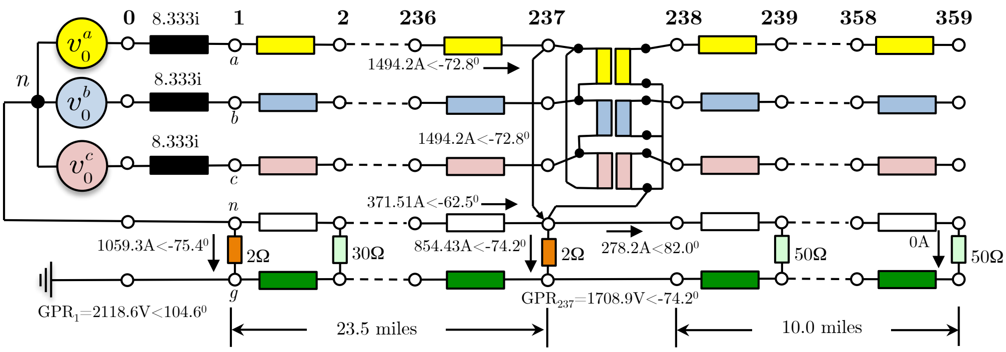

Figure 8: 115/12kV Test system - Fault current distribution (5x5 model)

References

[1] IEEE Guide for Safety in AC Substation Grounding, IEEE Std 80-2013, https://doi.org/110.1109/IEEESTD.2015.7109078

[2] A. P. Sakis Meliopoulos, Power System Grounding and Transients-An Introduction, Marcel-Dekker, New York, 1988.

[3] W. H. Kersting, Distribution system modeling and analysis, CRC press, Fourth Ed. 2018

[4] J.R. Carson, Wave propagation in overhead wires with ground return, BellSyst. Tech. J. 5 (October (4)) (1926) 539-554.

[5] F. Dawalibi, Ground fault current distribution between soil and neutral conductors, IEEE Trans. Power Appar. Syst. PAS-99 (March (2)) (1980) 452-461

[6] H. Gooi, S. Sebo, Distribution of ground fault currents along transmissionlines-an improved algorithm, IEEE Trans. Power Appar. Syst. PAS-104 (March(3)) (1985) 663-670.

[7] L.M. Popovic, A practical method for evaluation of ground fault currentdistribution on double circuit parallel lines, IEEE Trans. Power Deliv. 15 (1)(2000) 108-113.

[8] L. Levey, Calculation of ground fault currents using an equivalent circuit and a simplified ladder network, IEEE Transactions on Power Apparatus and Systems PAS-101 (8) (1982) 2491-2497.

[9] L. Levey, Computation of fault currents and voltages along a multi-grounded neutral power line having multiple phase conductors, IEEE Transactions on Power Delivery 6 (4) (1991) 1541-1548.

[10] F. Kiessling, P. Nefzger, J.F. Nolasco, U. Kaintzyk, Overhead Power Lines, Springer Berlin Heidelberg, Berlin, Heidelberg, 2003.

[11] P.L. Buccheri, S. Mangione, Analysis of ground fault current distribution alongnonuniform multi-section lines, Electr. Power Syst. Res. 78 (September (9))(2008) 1610-1618.

[12] J. Zou, J.B. Lee, J.J. Li, S. Chang, Evaluating ground fault current distribution on overhead transmission lines using an iterative nodal analysis, COMPEL-Int. J.Comput. Math. Electr. Electron. Eng. 30 (2) (2011) 622-640.

[13] D. R. R. Penido, L. R. de Araujo, M. de Carvalho Filho, (2015). A fault analysis algorithm for unbalanced distribution systems. IEEE Latin America Transactions, 13(1), 107-115.

[14] D. R. R. Penido, L. R. de Araujo, M. de Carvalho Filho, (2016). An enhanced tool for fault analysis in multiphase electrical systems. International Journal of Electrical Power & Energy Systems, 75, 215-225.

[15] D. Montenegro, M. Hernandez, G.A. Ramos, Real time OpenDSS framework for distribution systems simulation and analysis, In proc. IEEE/PES Transmission and Distribution: Latin America Conference and Exposition, pp. 1-5, 2012

[16] WinIGS Applications Guide, January 2004, available at http://www.apconcepts.com/_downloads/IGS_AGuide.pdf.

[17] CDEGS User manual, SES technologies, Montreal, 2005.

[18] J. Klucznik, Earth wires currents calculation by tableau analysis. Electr. Power Syst. Res., 151 (2017), 329-337

[19] J. Acharya, W. Xu, Ground potential rise of multi-grounded neutral and shield wires in joint systems, Electr. Power Syst. Res. 80 (9) (2010) 1074-1081.

[20] K. Oka, J. Yoshinaga, S. Koizumi, S. Uemura, Y. Ariga, Study of neutral grounding for 22 kV distribution systems, IEEE PES T&D Conference and Exhibition (3) (2002).

[21] J. Acharya, Y. Wang, W. Xu, Temporary overvoltage and ground potential rise characteristics of distribution feeders with multi-

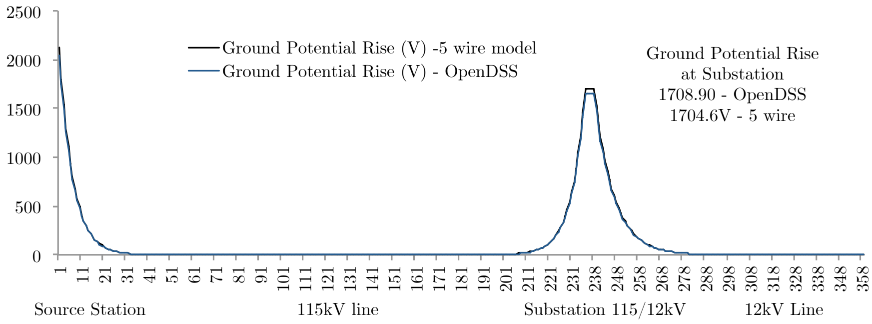

Figure 9: 115/12kV Test system - GPR profile

grounded neutral, IEEE Transactions on Power Delivery, 25 (2) (2010) 1036-1044

[22] T.H. Chen, W.C. Yang, Analysis of multi-grounded four-wire distribution systems considering the neutral grounding, IEEE Transactions on Power Delivery 16 (4) (2001) 710-716.

[23] P. M. Anderson, Analysis of faulted power systems, Vol. 445m New York: IEEE press, 1995

[24] R. M. Ciric, A. P. Feltrin, L. F. Ochoa, Power flow in four-wire distribution networks-general approach. IEEE Transactions on Power Systems, 18 (4) (2003) 1283-1290.

[25] R. M. Ciric, A. P. Feltrin, L. F. Ochoa, Power flow in distribution networks with earth return. International journal of electrical power & energy systems, 26(5) (2004) 373.380.

[26] P. M. De Oliveira-De Jesus, C. H. Antunes, A detailed network model for distribution systems with high penetration of renewable generation sources, Electr. Power Syst. Res., 161 (2018) 152-166. https://doi.org/10.1016/j.epsr.2018.04.005

[27] R. M. Ciric, L. F. Ochoa, A. Padilla-Feltrin, H. Nouri, Fault analysis in four-wire distribution networks. IEE Proceedings-Generation, Transmission and Distribution, 152 (6) (2005) 977.982.

[28] Ramos-Leanos, O., Naredo, J. L., Uribe, F. A., Guardado, J. L. (2017). Accurate and Approximate Evaluation of Power-Line Earth Impedances Through the Carson Integral. IEEE Transactions on Electromagnetic Compatibility, 59(5), 1465-1473.

[29] A. Deri, G. Tevan, A. Semlyen, and A. Castanheira, The complex ground return plane a simplified model for homogeneous and multilayer earth return, IEEE Trans. Power App. Syst., vol. PAS-100, no. 8, pp. 3686-3693, Aug. 1981.

[30] C. Dubanton, Calcul approche des parametres primaires et secondaires d'une ligne de transport. Valeurs homopolaires, EDF Bulletin de la Direction des Etudes et Recherches Serie B Reseaux Electriques, Materiels Electriques, vol. 6, pp. 53-62, 1969.

[31] F. L. Alvarado and R. Betancourt, An accurate closed-form approximation for ground return impedance calculations, Proc. IEEE, vol. 71, no. 2, pp. 279-280, Feb. 1983.

[32] T. Noda, A double logarithmic approximation of Carson's ground return impedance, IEEE Trans. Power Del., vol. 21, no. 1, pp. 472-479, Jan. 2006.

[33] Kersting, W. H. (2011). The whys of distribution system analysis. IEEE Industry Applications Magazine, 17(5), 59-65.

[34] Blackburn, J. L. (1993). Symmetrical components for power systems engineering. CRC Press.

[35] Pau, M., Pegoraro, P. A., Sulis, S. Efficient branch-current-based distribution system state estimation including synchronized measurements. IEEE Transactions on Instrumentation and Measurement, (2013) 62(9), 2419-2429.

[36] A. S. Meliopoulos, F. Zhang, Multiphase power flow and state estimation for power distribution systems. IEEE Transactions on Power Systems, 11(2) (1996) 939-946.

[37] A. S. Meliopoulos, G. Cokkinides, R. Huang, E. Farantatos, S.Choi, Y. Lee, X. Yu, Smart grid technologies for autonomous operation and control. IEEE Transactions on Smart Grid, 2(1) (2011) 1-10.

[38] IEEE Guide for the Application of Neutral Grounding in Electrical Utility Systems-Part I: Introduction. IEEE Std C62.92.1-2016.

[39] Kersting, W.H. A three-phase unbalanced line model with grounded neutrals through a resistance. In Proceedings of the 2008 IEEE Power and Energy Society General Meeting-PESGM, Pittsburgh, PA, USA, 20–24 July 2008; pp. 12651-12652.

Appendix A. OpenDSS script

```
! n=1 SHORT-CIRCUIT ANALYSIS November 15, 2018
! Full NEV approach (considering tower footings)
clear
New circuit.SOURCE_1    bus1=n1.1  bus2=n1.4
basekV=7.1996 pu=1 angle= 000
Z1=[.0000001, .0000001]  phase=1
New Vsource.SOURCE_2 bus1=n1.2  bus2=n1.4
basekV=7.1996 pu=1 angle=-120
Z1=[.0000001, .0000001]  phase=1
New Vsource.SOURCE_3 bus1=n1.3  bus2=n1.4
basekV=7.1996 pu=1 angle= 120
Z1=[.0000001, .0000001]  phase=1
set earthmodel=carson
new wiredata.conductor Runits=mi Rac=0.306 GMRunits=ft
GMRac=0.0244  Radunits=in
new wiredata.neutral     Runits=mi Rac=0.592 GMRunits=ft
GMRac=0.00814 Radunits=in
new linegeometry.4wire nconds=4 nphases=3 reduce=no
~ cond=1 wire=conductor units=ft x=-4    h=28
~ cond=2 wire=conductor units=ft x=-1.5 h=28
~ cond=3 wire=conductor units=ft x=3    h=28
~ cond=4 wire=neutral   units=ft x=0    h=24
new line.line1 geometry=4wire length=6000 units=ft
 bus1=n1.1.2.3.4 bus2=n2.1.2.3.4 Rho=100
!New Load.load1b.2 Phases=1  Bus1=n2.2.4   kVA=3500
pf=0.95   kV=12.47  conn=wye  vminpu=0.1 vmaxpu=1.9
!New Load.load1c.3 Phases=1  Bus1=n2.3.4   kVA=2500
 pf=0.85  kV=12.47 conn=wye vminpu=0.1 vmaxpu=1.9
New Reactor.SourceGround Phases=1 Bus1=n1.4 Bus2=n1.0 R=100.0
New Reactor.Load1Ground  Phases=1 Bus1=n2.4 Bus2=n2.0 R=100.0
set voltagebases=[12.47]
calcvoltagebases     ! **** let DSS compute voltage bases
New Fault.faseA   Phases=1  Bus1=n2.1  Bus2=n2.4
solve !.
show voltages LN Nodes
show currents resid=yes elements
```